Astron. Astrophys. 119, 61–68 (1983)

ASTRONOMY AND ASTROPHYSICS

Evolution of massive pregalactic stars

II. Nucleosynthesis in pair creation supernovae and pregalactic enrichment

W. W. Ober[1], M. F. El Eid[2], and K. J. Fricke[2]

[1] Max-Planck-Institut für Physik und Astrophysik, Karl-Schwarzschild-Strasse 1, D-8046 Garching bei München, Federal Republic of Germany
[2] Universitäts-Sternwarte Göttingen, Geismarlandstrasse 11, D-3400 Göttingen, Federal Republic of Germany

Received June 28, accepted October 14, 1982

Summary. The final evolution of Population III stars (zero metal stars) having large masses ($M \geqq 80\,M_\odot$) is considered. Stellar cores consisting mainly of carbon and oxygen obtained from quasistatic calculations are evolved through the e^-e^+-pair creation instability. Hydrodynamical computations of the collapse and the supernova explosion (pair creation supernova: PCSN) coupled to a network of nuclear reactions are presented. Carbon-oxygen core masses between 48 and $112\,M_\odot$ are found to explode, corresponding to an initial mass range $100 < M_i/M_\odot \lesssim 220\,M_\odot$. The nucleosynthesis products in PCSN due to incomplete explosive oxygen burning are calculated. Elements in the range carbon to calcium are produced, and no iron-peak elements result in the PCSN process. The enrichment of the pregalactic gas due to the combined effect of steady mass loss and the PCSN explosion is estimated. It appears that only a small fraction (about 10^{-4}) of the gas is processed through the Population III stars of large masses, if the resulting heavy element enrichment is constrained to the minimum metallicity ($\sim 10^{-5}$) observed in extreme Population II stars.

Key words: supernova explosions – massive stars – nucleosynthesis – pregalactic enrichment – cosmology

1. Introduction

In a previous work (El Eid et al., 1982; to be referred to as Paper I) the quasistatic evolution of Population III stars (zero metal stars) in the mass range 80–500 $M_\odot$ has been examined during the hydrogen and helium burning phases. In Paper I the mass-loss rates taken into account are in accord with those predicted from non-linear pulsational analysis. The effects of mass loss on the internal structure of the stellar models have been investigated, and relations between the initial masses and the helium core masses, as well as the carbon-oxygen masses were presented.

In this paper we investigate the stages of evolution beyond the helium burning. In the mass range under study the evolution toward carbon and oxygen burning proceeds exceedingly fast so that the stars do not restore thermal equilibrium. Instead the central parts of the stars evolve into the region of e^-e^+-pair creation, and the stars consequently encounter dynamical instability. The rapid carbon burning phase, the ensuing collapse, and the explosion phases of the stellar models obtained by the end of helium burning (see Paper I) have been followed by using a hydrodynamical code coupled to a network of nuclear reactions.

The aim of the present investigations is (i) to determine the mass range in which the evolution terminates explosively by the pair creation supernova (PCSN), (ii) to follow in a consistent way the nucleosynthesis which may occur in PCSN in order to assess the kind and level of the resulting enrichment. Fowler and Hoyle (1964) were the first to suggest that the pair creation instability may occur for massive stars.

Several calculations on the PCSN have used pure oxygen cores as initial models (Barkat et al., 1967; Fraley, 1969; Wheeler, 1977). None of these works has mapped out the mass range of explosion. Barkat et al. considered 30 and $40\,M_\odot$ oxygen cores. An explosion was found in the second case, while the first exhibits relaxation oscillations. Frayley's calculations were done for oxygen cores of 45, 52, and $60\,M_\odot$. Oscillations occurred in the $45\,M_\odot$ case and about $2\,M_\odot$ were expelled, while the other cores exploded totally. Wheeler's results have shown that oxygen cores of 10^3 and $10^4\,M_\odot$ collapse to black holes with no mass ejection.

Another type of investigations (Rakavy and Shaviv, 1968; Bond et al., 1982) are based on using the dimensionless entropy to characterize the collapse trajectories and so to follow the oxygen core evolution.

Finally, Arnett (1973) evolved helium stars of 64 and $100\,M_\odot$, which he related to 58 and $93\,M_\odot$ oxygen cores. Both stars exploded, but a $2.2\,M_\odot$ silicon remnant results in the $64\,M_\odot$ case. Woosley and Weaver (1982) considered C/O cores with ^{16}O in 2:1 relation to ^{12}C having 60, 80, 100, and $200\,M_\odot$. Explosions were found, apparently with no remnant, for the 60, 80, and $100\,M_\odot$ cores. Weaver and Woosley estimate that the critical mass for black hole formation is $300\,M_\odot$ for stars evolving without mass loss. The semi-analytical considerations of Bond et al. (1982) suggest a lower limit of $100\,M_\odot$ for the oxygen core mass.

In Sect. 2 of this paper the overall results of the final phases of the Population III stars are described, and the mass range of PCSN is presented. Section 3 contains a summary of the nucleosynthesis in PCSN. In Sect. 4 an estimate of the pregalactic enrichment is given. Our conclusions follow.

2. The final fate of very massive Population III stars

As we have shown in Paper I, the Population III stars at the end of helium burning consist mainly (over 90%) of carbon and oxygen with a thin envelope of mostly helium. Therefore in the following we call them C/O cores.

The evolution of C/O cores has been followed using stellar models from the quasi-static calculations (those at the end of

Send offprint requests to: K. J. Fricke

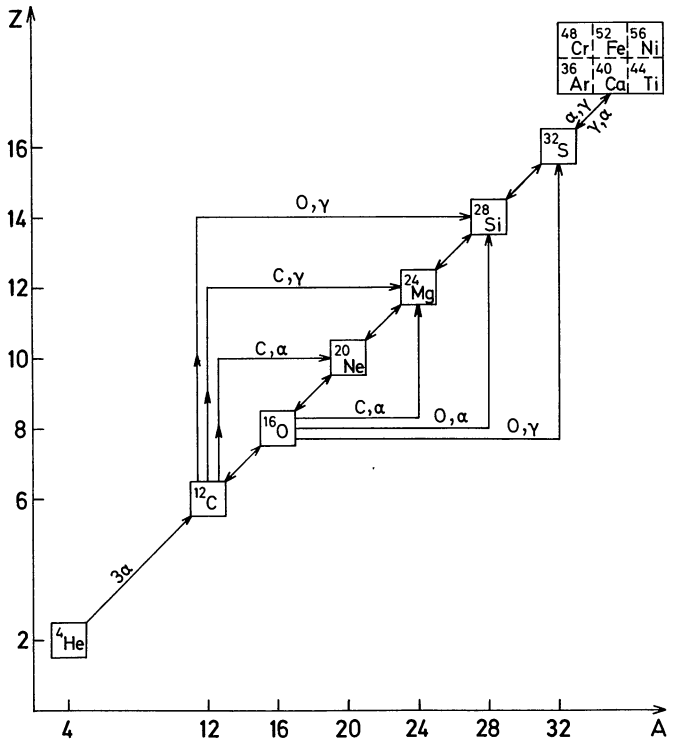

Fig. 1. A simplified network of nuclear reactions. The (α,γ) and (γ,α) reactions link ^{12}C to the iron-group. The triple-alpha is shown schematically, and the heavy-ion reactions $^{12}C+^{12}C$, $^{12}C+^{16}O$, and $^{16}O+^{16}O$ are illustrated

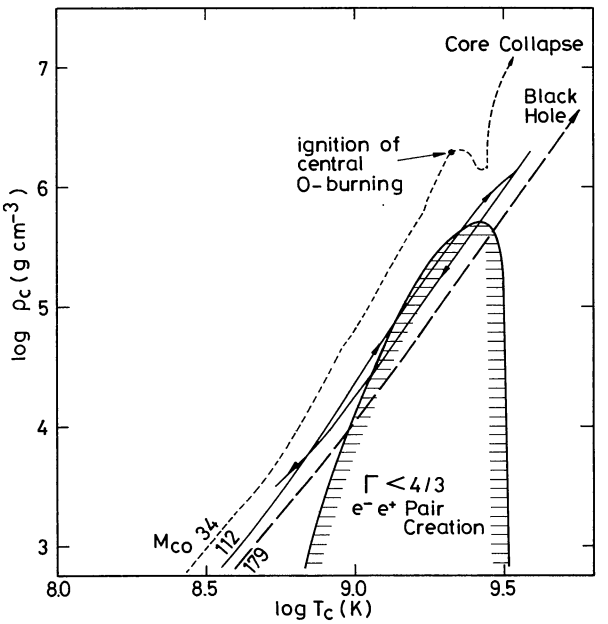

Fig. 2. The ϱ_c-T_c-diagram for C/O cores of 34, 112, and 179 $M_\odot$. The hatched curve encloses the domain of pair creation instability where the adiabatic index $\Gamma<4/3$

helium burning) as initial models for the subsequent phases. An implicit hydrodynamical code has been constructed which integrates the equations of conservation of energy, mass, and momentum assuming spherical symmetry.

The effect of electron-positron pair creation (e^-e^+-pairs) on the equation of state is taken into account by numerically evaluating the general expressions (cf. e.g. Cox and Giuli, 1968) for an equilibrium mixture of e^-, e^+ and photons. Neutrino energy losses due to the photoneutrino process, the pair neutrino process and the plasma neutrino process (cf. Beaudet et al., 1967) were also taken into account. The nucleosynthesis has been followed by a network of nuclear reactions, consisting of 13 nuclei linked by 29 main reactions, including heavy-ion reactions (Fig. 1). The reaction rates are taken from the compilations of Fowler et al. (1975).

The instability region caused by e^+e^--pair creation has been determined by calculating the adiabatic index $\Gamma\equiv(\partial\ln p/\partial\ln\varrho)_{ad}$ using the relation

$$\Gamma=\frac{\varrho}{p}\left\{\left(\frac{\partial p}{\partial\varrho}\right)_T+\frac{1}{\varrho^2}\left[\left(\frac{\partial p}{\partial T}\right)_\varrho\right]^2\Big/\left(\frac{1}{T}\left(\frac{\partial\varepsilon}{\partial T}\right)_\varrho\right)\right\},$$

where ϱ is the density, p is the total pressure, and ε denotes the internal energy per gram. In Fig. 2 the region of instability ($\Gamma<4/3$) is shown in a T-ϱ plane. Dynamical instability occurs when a sufficiently large part of the core (about 30% mass) has entered that region.

At the point of carbon ignition ($T_8\sim9$) the contraction velocities are still negligibly small but increase rapidly afterwards to 1 km s^{-1} when the dynamical terms become important and collapse sets on. The central temperatures (T_i), and densities (ϱ_i) at this stage are contained in Table 1 for the indicated masses.

The early phase of collapse proceeds nearly homologously with $(\partial\ln T/\partial\ln\varrho)\sim1/3$ due to the high velocity of sound ($v_s\sim10^9$ cm/s). In a time of the order of 100 s (50 to 100 free-fall time scales) infall velocities in excess of 10^3 km s^{-1} are attained. Figure 3 shows evolution of the velocity profile for the case of the 112 $M_\odot$ core (initial mass of 200 $M_\odot$). During collapse the central temperatures and densities rise well above $T=3\,10^9$ K and $\varrho=10^5$ g/cm^3 (for details see the entries T_{max} and ϱ_{max} in Table 1). Under such conditions oxygen burns explosively with a nuclear energy release $E_{nuc}\gtrsim10^{52}$ erg. A deflagration wave is initiated at the center, which propagates outwards at subsonic velocity.

Because of the strong temperature dependence of the thermonuclear reactions, the collapse is first stopped at the center, but the velocities of the loosely bound outer layers become as large as 13,000 km s^{-1}, when the deflagration wave reaches the steep density gradient near the surface of the core.

It is important to find out the mass range in which explosive oxygen burning leads to explosion. An example of our calculations is shown in Fig. 4, which displays a T-ϱ profile of a 112 $M_\odot$ C/O core at the time of collapse reversal. A large part of the core is still located within the instability region when explosive oxygen burning is able to reverse the collapse and, finally, disrupt the whole core. Figure 2 illustrates the central evolution of the 112 $M_\odot$ core during collapse and explosion in a $T_c-\varrho_c$-diagram. As indicated in the same figure, the 179 $M_\odot$ core undergoes total collapse, while the 34 $M_\odot$ core avoids the pair instability region. The summary of our results in Table 1 indicates explosions for all cores of 60, 78, 100, and 112 $M_\odot$.

In the case of higher core masses the collapse proceeds to higher T_c and ϱ_c before the nuclear energy release affects the collapse. Consequently, at temperatures in excess of $4\,10^9$ K endothermic photodissociation of heavy elements mainly into the α-channel will be effective in reducing the internal energy density and the pressure. The effect will be continuing collapse.

Table 1. Results of the collapse and explosion calculations. M_i and M_f are the initial mass and the actual mass at helium exhaustion. (T_i, ϱ_i) denote the temperature (in units of 10^9 K), and density at the onset of the collapse, while (T_{max}, ϱ_{max}) are those at reversal of collapse. E_{inf} is the kinetic energy during infall, while E_{ex} the kinetic energy during expansion. V_{ex} denotes the maximum expansion velocities during explosions. Numbers in brackets are power of ten

$M_i/M_\odot$	108	124	150	184	200	220	300
$M_f/M_\odot$	50	60	78	100	112	125	179
$T_{9,i}$	1.61	1.54	1.35	1.57	1.50	1.40	1.29
ρ_i/g cm^{-2}	7.55(4)	5.77(4)	3.00(4)	1.65(5)	1.00(5)	7.00(4)	2.7(4)
$T_{9,max}$	2.68	3.55	3.18	3.55	3.91	---	---
ρ_{max}/g cm^{-3}	1.38(6)	1.27(6)	5.80(5)	1.72(6)	1.95(6)	---	---
E_{inf}/km s^{-1}	8.25(48)	3.37(50)	3.19(50)	6.91(50)	2.44(51)	>4.(51)	>3.(52)
E_{nuc}/erg	1.86(51)	7.85(51)	1.30(52)	1.66(52)	5.60(52)	∿1.(52)	∿1.(52)
V_{ex}/km s^{-1}	2080	8480	9730	10700	13000	---	---
E_{ex}/erg	1.60(50)	1.32(52)	1.50(52)	2.98(52)	4.40(52)	---	---
Mass of oxygen burned	---	9.24	5.30	12.7	25.3	---	---
Fate	explosive mass loss	explosion	explosion	explosion	explosion	collapse	collapse

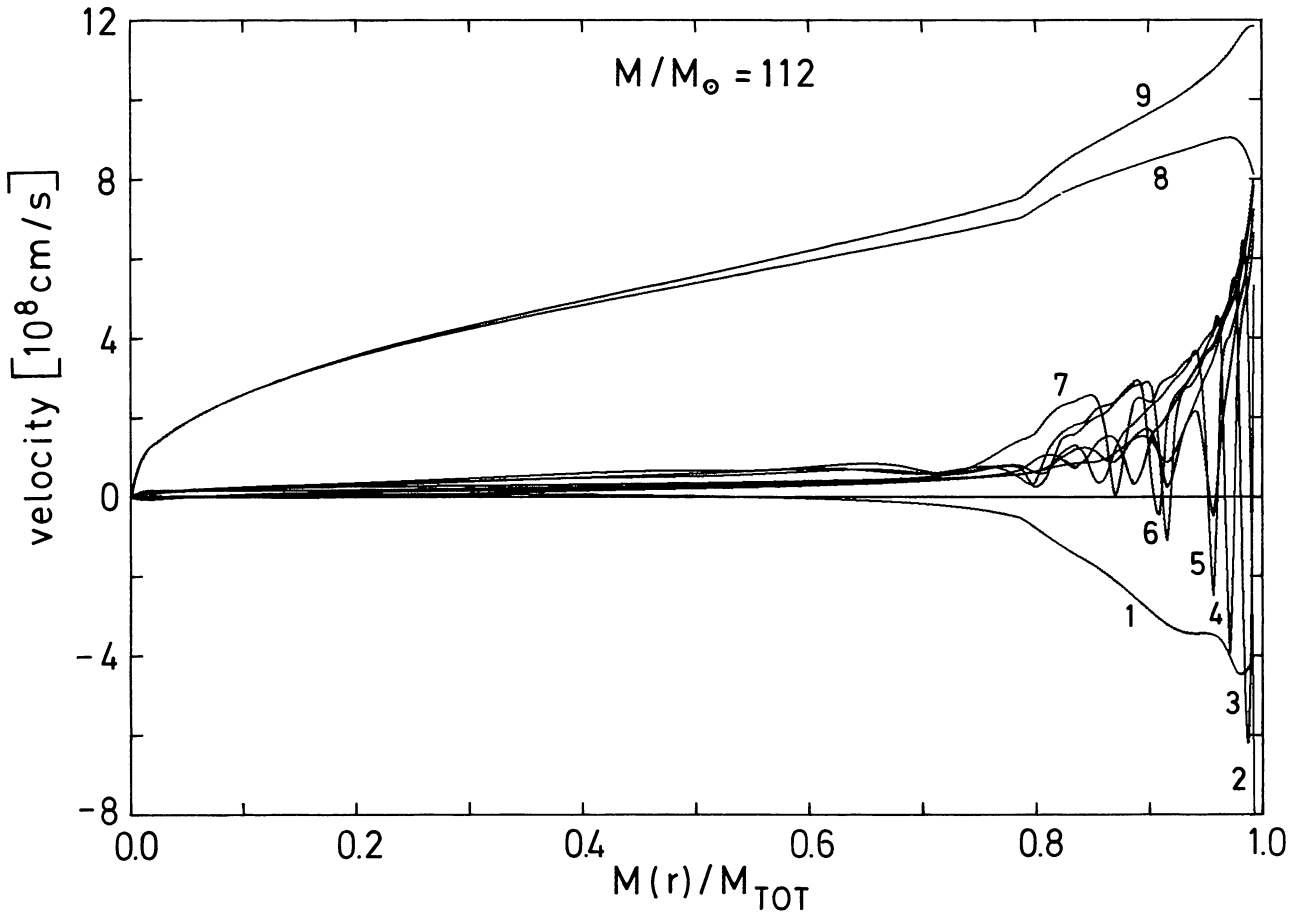

Fig. 3. The change of the velocity profile in time for the case of the 112 $M_\odot$ core (initial mass of 200 $M_\odot$). $M(r)/M$ represents the mass coordinate. The numbers indicate the time after the onset of the collapse in seconds: *1* 222, *2* 234.5, *3* 235.7, *4* 236.7, *5* 237.8, *6* 239.9, *7* 241, *8* 354, *9* 612. The core is disrupted without leaving a remnant (see text)

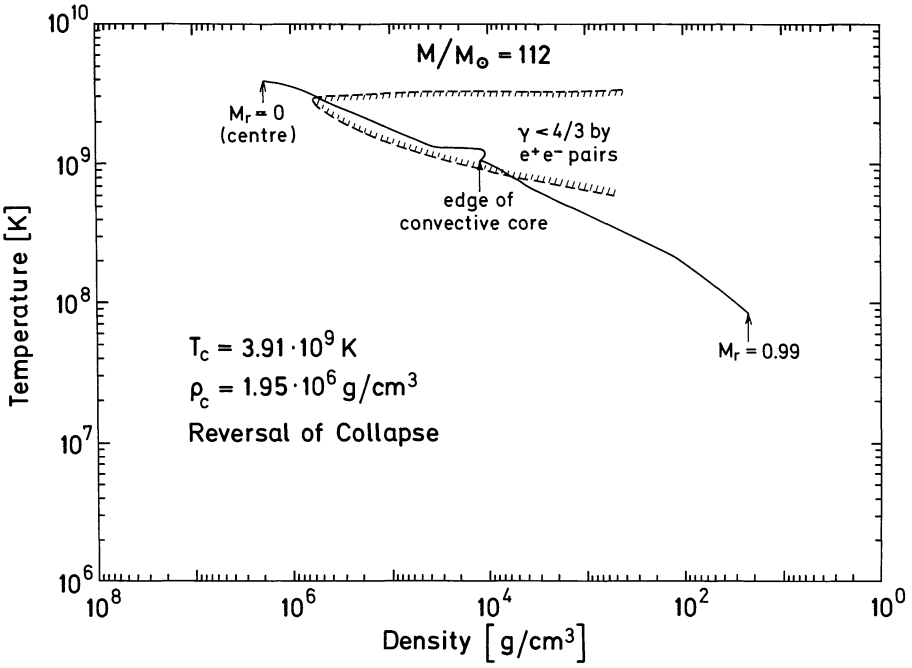

Fig. 4. The T-ϱ profile for a $112\,M_\odot$ core at the time of reversal of the collapse. The central temperature T_c, and density ϱ_c are indicated

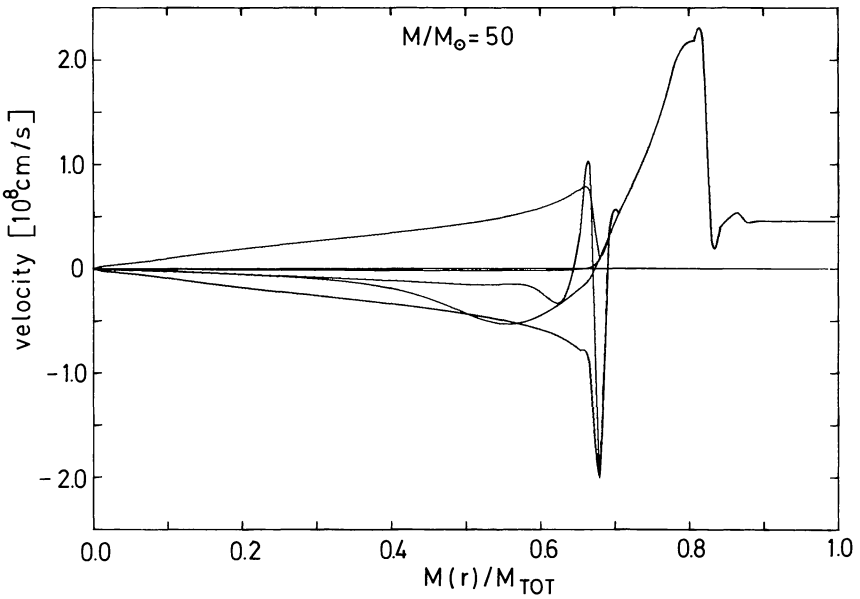

Fig. 5. The velocity profile of the $50\,M_\odot$ core is shown. The successive mass ejections are illustrated by the outer 18% of the mass, whereas the matter in the region between the mass fraction 0.68 and 0.82 is expelled at higher velocity (see text). A very sharp boundary developes at the interface of the two shells. The remaining core ($34\,M_\odot$) undergoes relaxation oscillations

Calculations for $125\,M_\odot$ and $179\,M_\odot$ cores did not show explosions. Instead the oxygen fuel was entirely consumed, and temperatures beyond $6\,10^9$ K were reached. Thus, such objects will collapse towards black holes.

The lower mass cores display a different behaviour. Those of $34\,M_\odot$ (initially $80\,M_\odot$) and $46\,M_\odot$ (initially $100\,M_\odot$) do not become pair-unstable. However, they develop a kind of relaxation oscillations with continuing contraction. Their evolution beyond oxygen ignition has not been followed, but it will probably proceed through the subsequent burning stages. According to Arnett's calculations (Arnett, 1972; see also Arnett and Schramm, 1973), a helium core with mass $M_\alpha = 32\,M_\odot$ would collapse after the formation of an Fe–Ni core slightly more massive than the Chandrasekhar limit. Since we found a similar evolution for our $80\,M_\odot$ star to that of an $M_\alpha = 32\,M_\odot$ core through helium burning (cf. Paper I), we conclude that stars of $M < 100\,M_\odot$ do not reach pair instability.

An interesting behaviour has been found in the case of a $50\,M_\odot$ core. This object showed explosive mass loss in two events. First, at $T_c \sim 1.6\,10^9$ K and $\varrho_c \sim 7.5\,10^4$ g/cm^3 it began to collapse, but the velocities did not exceed 400 km s^{-1}. Due to the homologous nature of the collapse, the loosely bound helium-rich surface layers were heated up above 10^9 K, which initiated violent He-burning. The nuclear energy release ($\sim 1.5\,10^{49}$ erg) could stop the mild collapse, resulting in the ejection of $9\,M_\odot$. Secondly, the remaining object ($41\,M_\odot$) recollapsed, and at $2.68\,10^9$ K rapid Ne-burning and the onset of O-burning led the collapse to stop again. This time $7\,M_\odot$ were ejected, but the explosion was not strong enough to disrupt the whole object.

In Fig. 5 the velocity profile of the $50\,M_\odot$ core is shown. The successive mass ejections are clearly illustrated by the outer 18% of the mass expanding at 500 km s^{-1} and another 14% with 2000 km s^{-1}. Figure 6 shows the $T-\varrho$ profiles versus stellar mass at the onset of collapse and for the last calculated model. The

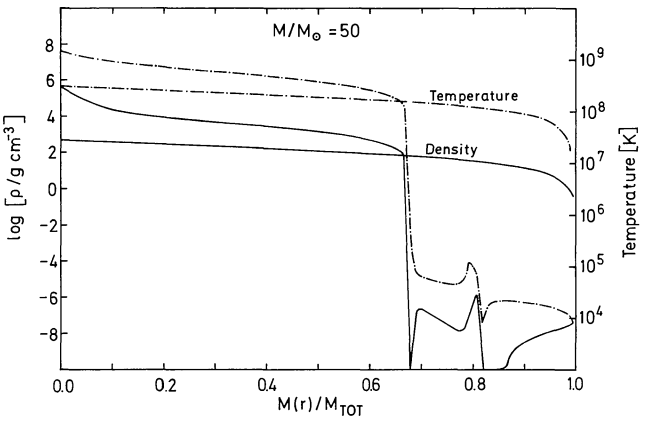

Fig. 6. The T-ϱ profile for the $50\,M_\odot$ core at the onset of collapse and for the last calculated model. The remaining object of $34\,M_\odot$ is very compact having a radius of $2\,10^{10}$ cm

remaining object of about $34\,M_\odot$ is very compact with a radius of $2\,10^{10}$ cm; its fate is unclear, probably it will evolve through subsequent nuclear burning phases.

The results of the present hydrodynamical calculation are also summarized in Table 1. Based on our hydrodynamical computations we find PCSN to occur in the carbon-oxygen core mass range $48 < M_{\rm core}/M_\odot \leqq 112$. On the basis of our quasistatic evolutionary calculations, with the mass loss rate adopted therein (cf. Paper I), this range of core masses corresponds to a stellar mass range from 50 to $120\,M_\odot$ at helium exhaustion and to a range of initial stellar masses M_i from 108 to $220\,M_\odot$.

It is intriguing that the semi-analytical investigations of Bond et al. (1982) suggest an upper mass limit for the PCSN of $M_{\rm CO}/M_\odot \simeq 100$, and $M_i/M_\odot > 220$.

3. Nucleosynthesis in PCSN

For stars of mass larger than $100\,M_\odot$ the carbon burning phase proceeds on a time scale of the order of 1 yr. The carbon is completely transformed to neon and magnesium. At central temperatures $T_c \gtrsim 2\,10^9$ K photo-dissociations of ^{20}Ne result in ^{16}O and ^{24}Mg. At higher T_c magnesium photodissociates too and, together with the onset of extensive oxygen burning, substantial amounts of ^{28}Si, ^{32}S, ^{36}Ar, and ^{40}Ca are synthesized. At $T_c \gtrsim 3\,10^9$ K explosive O-burning leads to the formation of a nearly pure silicon core. The energy release amounts to more than 10^{52} erg, within less than 20 s for the exploding cores between 50 and $125\,M_\odot$.

In Fig. 7 the chemical composition for a C/O core of $112\,M_\odot$ just after the explosion is illustrated. The innermost part (5% by mass) has been transmuted by Si-burning to ^{32}S, ^{36}Ar, and ^{40}Ca, and various burning phases can be identified. Due to the initially homologous collapse, the He envelope has been heated up beyond

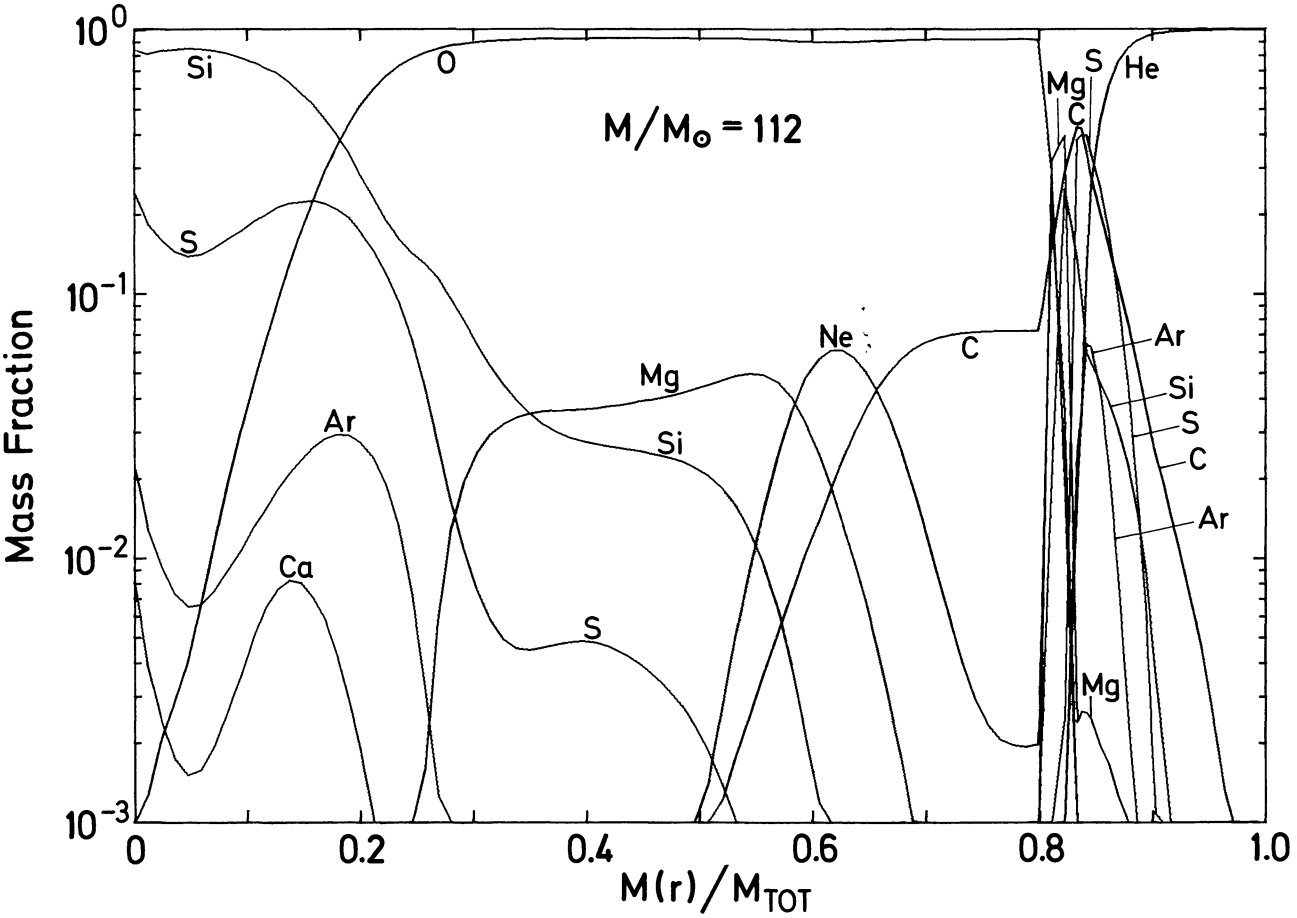

Fig. 7. The chemical composition for the $112\,M_\odot$ core after explosion. The various nuclear burning sites are shown. Silicon burning occurred in the innermost part (5%) of the mass. O-burning was efficient in about 30% of the mass. For $M(r)/M = 0.78$ to 0.83 explosive He-burning has taken place (see text)

Table 2. Composition of ejected PCSN matter. M_f is the actual mass at helium exhaustion

$M_f/M_\odot$	50[a]	60	78	100	112
He	0.049	0.048	0.044	0.147	0.142
C	0.042	0.046	0.039	0.030	0.023
O	0.190	0.606	0.692	0.640	0.538
Ne	0.018	0.045	0.034	0.016	0.009
Mg	0.020	0.071	0.084	0.034	0.020
Si	–	0.140	0.085	0.095	0.188
S–Ca	–	0.043	0.021	0.038	0.080

[a] Explosive mass-loss only, no total disruption

Table 3. Enhancement factors of products of explosive oxygen burning relative to the sun for three model calculations

Species	$X_*/X_\odot$ This work	Woosley and Weaver (1982)	Arnett and Schramm (1973)
^{1}H	0.02	–	–
^{4}He	0.46	1.55	0.34
^{12}C	6.85	24.90	5.2
^{14}N	3 (−4)	0.14	–
^{16}O	65.14	51.80	54.2
^{20}Ne	6.14	18.70	2.2
^{24}Mg	41.90	77.7	40.7
^{28}Si	300.26	207.2	
^{32}S	199.79	145.1	517.6[a]
^{36}Ar	67.13	72.5	
^{40}Ca	13.69	98.4	
Ejected ^{16}O mass fraction	0.538	0.43	0.45
$M_\alpha/M_\odot$	96	140	100
Population	III	III	Helium star

[a] Enhancement of Si through Ca nuclei

10^9 K, so that violent He-burning has occurred in a region $M(r)/M = 0.78$ to 0.83. Thus some Si and S are produced outside the convective core in this peculiar nucleosynthesis process.

Table 2 exhibits the composition of ejected matter in PCSN's. The amount of elements beyond magnesium increases in general with stellar mass, while the oxygen content decreases because of the higher central temperatures achieved during collapse. No significant amounts of nuclear species beyond ^{40}Ca are produced in the most massive PCSN's.

Another point of interest is the lack of neutron-rich isotopes, which is related to the underproduction of ^{14}N in this extremely metal-deficient CNO-cycle. If one, however, were to ignore mass loss during He-burning, then some ^{14}N may be produced by convective mixing as has been argued by Woosley and Weaver (1982).

In Table 3 the enhancement factors over solar abundances of various nuclear species are compared to the calculations of Woosley and Weaver (1982) for a $200\,M_\odot$ Population III star (without mass loss) and the results for a helium star with $M_\alpha = 100\,M_\odot$ by Arnett and Schramm (1973) (see also Arnett, 1973). The enhancement factor of 52–65 (Table 3) for oxygen indicates that only a small fraction of matter could have experienced conditions as reached by a $200\,M_\odot$ primordial star. In general, our results in Table 3 are closer to Arnett's than to those of Woosley and Weaver. This is understandable, since our quasistatic calculations with mass loss as described in Paper I resemble in many respects the evolution of the cores discussed by Arnett.

4. Pregalactic enrichment

In this section we estimate the enrichment of the pregalactic medium by Population III stars with $M > 80\,M_\odot$, which finally explode or collapse. The pregalactic gas is already slightly contaminated by the mass lost during the quasistatic evolution. Most of the enrichment is, however, found to be due to the matter ejected in the PCSN process.

We assume that a fraction p of the protogalactic cloud goes into stars. The free parameter p is constrained by the minimum metallicity $Z_{\min}$ of the order of 10^{-5} as observed in extreme Population II stars (Ake and Greenstein, 1980). Because of the lack of better knowledge, the spectrum of pregalactic stars is as usually taken to be a power law:

$$N(M)dM \propto M^{-n}dM\,, \quad (M_l < M < M_u)\,,$$

where $N(M)$ is the number of stars in the mass interval $(M, M+dM)$ and M_l is the lower and M_u the upper cut-off in the spectrum. There are observational and theoretical reasons (cf. Carr et al., 1982) which suggest that n may be smaller than the Salpeter slope 2.35 at low metallicity. Therefore we also calculate for comparison the enrichment using $n=2.0$ and $n=1.8$ besides the standard value.

For an assessment of the primordial metal enrichment we only need to consider the mass range $108 < M_i/M_\odot < 220$ in which PCSN explosions occur. This corresponds – according to our quasistatic evolutionary sequences – to the range of carbon-oxygen core masses $48 \lesssim (M_{\rm core}/M_\odot) \lesssim 112$. Primordial stars below our lower mass limit if they have been formed at all must be extremely rare. Otherwise they would have contaminated the pregalactic medium through their supernova type II explosions.

In this sense the lower mass limit may be justified by the extremely low metallicity observed in the oldest Population II stars (the so-called G-dwarf problem). There is also evidence that these stars belong to the secondary (or even later) generation as they contain s-process elements in their envelopes (Truran, 1980). A lower mass limit of the order of $100\,M_\odot$ is also supported by the consideration of star formation in a medium devoid of metals and exposed to an enhanced background radiation (cf. Carr et al., 1982). All stars between our lower mass limit and the maximum mass for which a stable main sequence stage exists contribute to the enrichment (mainly with helium) by steady mass loss. The upper mass limit for steady enrichment will therefore be $M_u = 8\,10^4\,M_\odot$, beyond which the post-Newtonian instability prevents a static main sequence evolution (Fricke, 1973). The effect of exploding (cf. Ober, 1979) and/or collapsing supermassive stars with masses $M > M_u$ on the enrichment and the mass budget is likely to be small and will be ignored in the following.

The total mass of the stars which contribute to the enrichment is then

$$M_* = a \int_{M_l}^{M_u} m^{1-n}dm \equiv a\gamma\,. \tag{4.1}$$

Table 4. Enrichment of various elements by Population III stars. n is the slope of the IMF. A value 10^{-3} has been assumed for the efficiency parameter p. The results scale roughly with p for $p<10^{-2}$

n	He	C	N	O	Ne	Mg	Si	S→Ca	ΔZ	$\Delta X_{He}/\Delta Z$
2.35	3.0(−5)	4.0(−6)	<1.0(−10)	7.2(−5)	2.9(−6)	6.4(−6)	1.6(−5)	5.8(−6)	1.1(−4)	0.28
2.0	1.3(−5)	1.5(−6)	<1.0(−10)	2.7(−5)	1.1(−6)	2.3(−6)	5.9(−6)	2.3(−6)	4.0(−5)	0.32
1.8	1.1(−5)	7.5(−7)	10^{-10}	1.3(−5)	5.8(−7)	1.2(−6)	3.1(−6)	1.1(−6)	2.0(−5)	0.55

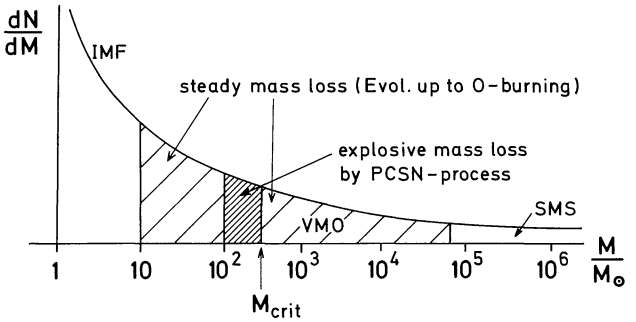

Fig. 8. A schematic representation of the initial mass function (IMF) and of different mass-ranges to pregalactic enrichment

Prior to star formation the mass in the form of a species j having the initial mass fraction X_j^0 is $M_0 X_j^0$, where M_0 is the initial mass of the cloud. As a consequence of primordial star formation, a fraction $M_* \cdot X_j^0$ is removed from the gas. In the following we denote by $R_W(m)$ and $R_{SN}(m)$ the fraction of matter returned to the gas by stellar wind and PCSN explosion, respectively. Then the mass in the form of the species j in the debris of the primordial stars is

$$M_j=(M_0-M_*)X_j^0+a\int_{M_l}^{M_u} R_W(m)X_j^W(m)m^{1-n}dm + a\int_{M_l}^{M_u} R_{SN}(m)X_j^{SN}(m)m^{1-n}dm, \quad (4.2)$$

where $X_j^W(m)$ and $X_j^{SN}(m)$ are the mass fractions in the gas resulting from stellar wind and PCSN explosions, respectively, and complete mixing of the ejected material in the cloud is assumed. Since no compact remnants are found in our calculations the quantity $R_{SN}(m)$ may be written as $R_{SN}(m)=\delta(m)\,(1-R_W(m))$ where $\delta(m)$ is unity for the mass range in which PCSN occurs (cf. Table 1) and zero otherwise.

The mass of the cloud left behind ofter the Population III generation is

$$M_1=M_0-M_*+\int_{M_l}^{M_u}(R_W(m)+R_{SN}(m))m^{1-n}dm \equiv M_0-M_*+aI_1 \quad (4.3)$$

and the enrichment of a species j is

$$\Delta X_j=\frac{M_j}{M_1}-X_j^0 = \frac{a}{M_1}\int_{M_l}^{M_u}[(X_j^W-X_j^0)R_W(m)+(X_j^{SN}-X_j^0)R_{SN}]m^{1-n}dm\equiv\frac{a}{M_1}I_2^j. \quad (4.4)$$

In particular the enrichment of a species j due to stellar wind alone is obtained by putting $R_{SN}=0$ in the expressions (4.3) and (4.4).

The dependence of ΔX_j on the parameter p, which fixes the amount of matter processed in primordial stars, is from the definition $p=M_*/M_0$ and from Eqs. (4.3) and (4.4)

$$\Delta X_j=\gamma p I_2^j\frac{1}{1+p(\gamma I_1-1)}. \quad (4.5)$$

This relation shows that ΔX_j does not in general scale with p. However, the numerical evaluation of Eq. (4.5) shows that for $p<10^{-2}$, to very good accuracy, $\Delta X_j \propto p$. The results for the combined effect of steady mass loss and PCSN explosions on the enrichment are summarized in Table 4 for $n=2.35$, $n=2.0$, and $n=1.8$ assuming $p=10^{-3}$.

The enrichment in He indicated in Table 4 is entirely due to the steady mass loss during the evolution prior to the final explosion of the primordial stars, the matter ejected in the explosion itself being deficient in He (cf. Table 3). The enrichment for He is subject to great uncertainty as the relative number of very high mass stars between 300 and $8\,10^4 M_\odot$ and their contribution to the mass lost are not well known. We estimate an uncertainty of 50–100% for ΔX_{He}.

The enrichment in helium relative to the total enrichment by heavy elements $\Delta X_{He}/\Delta Z$ ~0.28 to 0.55, which is one order of magnitude below the observed value for this quantity in HII regions (Peimbert and Torres-Peimbert, 1977). Most of the astrated helium can therefore not be explained by this process but has its origin in less massive stars of Populations I and II.

As to the absolute value of ΔZ, we note that the observed upper limit for Z in the oldest stars is $\sim 10^{-5}$. Constraining ΔZ in Table 4 to this bound implies that the efficiency p of primordial star formation in the mass range appropriate for PCSN explosions cannot have exceeded $\sim 2\,10^{-4}$.

Most of the enrichment in heavy elements occurs in the form of ^{16}O (~60%) and ^{28}Si (~14%) while the other metals up to Ca each contribute only a few percent at most. This is characteristic of the explosive oxygen burning taking place in PCSN's.

5. Summary and conclusions

In this paper we have simulated the final dynamical evolution of primordial stars of masses higher than $80 M_\odot$. We started from the models at the end of the quasistatic evolution with mass loss, obtained in Paper I. We find that within the mass range $108<M/M_\odot<220$, corresponding to C/O-cores of $48<M/M_{core}<112$, primordial stars explode as PCSN's leaving no compact remnants behind. The disruption of these stars is due to incomplete explosive oxygen burning (cf. Table 1). The mass ranges for PCSN's and the very massive stars (VMO's) of Paper I are demonstrated schematically in Fig. 8. Most of the heavy element enrichment from carbon to calcium is achieved by the exploding stars. No iron group elements are produced in this astrophysical site, in accordance with earlier results on exploding C/O-cores by Barkat et al. (1967). As Ober (1979) and Fricke et al. (1980) suggest, iron group elements might, however, be copiously produced by exploding stars in an even more extreme mass range

– by the relativistically unstable supermassive stars (SMS's) beyond $8\,10^4\,M_\odot$ which are also indicated in Fig. 8. The He-enrichment is insignificant and entirely due to mass loss during the slow phases of evolution.

The well-known "G- and K-dwarf problem" in the galactic disk (cf. Pagel and Patchett, 1975; Audouze and Tinsley, 1976) and in the galactic halo (Bond, 1981) concerns the fact that there are no stars found in these regions of the galaxy with a metal content below a certain minimum value $Z_{\min}=\zeta Z_\odot$, where $\zeta\sim 0.1$ in the disk and $\zeta\sim 10^{-3}$ in the halo. Pregalactic nucleosynthesis at the same time is constrained by and provides a solution for the G-dwarf problem in the galactic halo. We merely have to postulate (cf. Table 4) that the fraction $p\approx 0.2\zeta = 2\,10^{-4}$ of primordial matter has participated in PCSN explosions of Population III stars.

The composition of the ejected and mixed material has several features which compare favourably with abundance determinations in old stars: (i) the oxygen enhancement found here corroborates the interpretation of Sneden et al. (1979) – that a large fraction of oxygen has been produced earlier than the other heavy elements. (ii) The enrichment of elements from sulfur to calcium partially removes the difficulty that SN II explosions apparently underproduce these elements (Woosley and Weaver, 1982). (iii) As shown in Sect. 4 the α-particle nuclei in the same atomic mass range are found to be enhanced – a fact which finds some support from observations of metal poor stars (Peimbert, 1974). (iv) The presence of these nuclei in the matter processed by PCSN explosions implies that possibly only a single further generation of stars is needed for the formation of *s*-process elements which indeed are observed in the most metal-poor stars (Truran, 1980).

A problem exists with nitrogen. From our evolution and nucleosynthesis calculations for stars between 80 and $300\,M_\odot$ nitrogen is found to be strongly underproduced presumably due to the absence of convective dredge-up or overshooting. Primary production of nitrogen may, however, occur in higher mass primordial stars as has been suspected in the case of a $500\,M_\odot$ Population III star by Woosley and Weaver (1982). The possible presence of nitrogen in very old stars (Barbury, 1981) could then partly be understood in terms of such objects.

Acknowledgement. We gratefully acknowledge support of this investigation by the Deutsche Forschungsgemeinschaft under grants Fr 325/9 and Fr 325/14. The authors thank B. J. Carr for many critical remarks.

References

Ake, T.B., Greenstein, J.L.: 1980, *Astrophys. J.* **240**, 859
Arnett, W.D.: 1972, *Astrophys. J.* **176**, 681 and 699
Arnett, W.D., Schramm, D.N.: 1973, *Astrophys. J.* **184**, L 47
Arnett, W.D.: 1973, in *Explosive Nucleosynthesis*, eds. W.D. Arnett and D.N. Schramm, Univ. of Texas Press, Austin
Audouze, J.M., Tinsley, B.M.: 1976, *Ann. Rev. Astron. Astrophys.* **14**, 43
Barbuy, B.: 1981, Thèse de Doctorat d'Etat, Université de Paris-VII
Beaudet, G., Petrosian, V., Salpeter, E.E.: 1967, *Astrophys. J.* **150**, 979
Bond, H.E.: 1981, *Astrophys. J.* **248**, 606
Bond, J.R., Arnett, W.D., Carr, B.J.: 1982, in *Supernovae: A Survey of Current Research*, eds. M.J. Rees and R.J. Stoneham, Reidel, Dordrecht, p. 303
Carr, B.J., Bond, J.R., Arnett, W.D.: 1982, Proceedings of the ESO Workshop on "The Most Massive Stars", eds. D'Odorico et al., Garching, Germany
Cox, J.P., Giuli, R.T.: 1968, Principle of Stellar Structure, Vol. II, Gordon and Breach, New York
El Eid, M.F., Fricke, K.J., Ober, W.: 1983, *Astron. Astrophys.* **119**, 54 (Paper I)
Fowler, W.A., Hoyle, F.: 1964, *Astrophys. J. Suppl. Ser.* **9**, 201
Fowler, W.A., Caughlan, G.R., Zimmermann, B.: 1975, *Ann. Rev. Astron. Astrophys.* **13**, 69
Fraley, G.S.: 1968, *Astrophys. Space Sci.* **2**, 96
Fricke, K.J.: 1973, *Astron. Astrophys.* **183**, 941
Fricke, K.J., Ober, W., Woosley, S.E.: 1980, Proceedings 9th Texas Symp., New York, p. 399
Ober, W.W.: 1979, in *Les Houches XXXII-Physical Cosmology*, eds. Balian et al., North-Holland, Amsterdam
Pagel, B.E.J., Patchett, B.E.: 1975, *Monthly Notices Roy. Astron. Soc.* **172**, 13
Peimbert, M.: 1974, in *The Formation and Dynamics of Galaxies*, IAU *Symp.* **58**, 141
Peimbert, M., Torres-Peimbert, S.: 1977, *Monthly Notices Roy. Astron. Soc.* **179**, 217
Rakavy, G., Shaviv, G.: 1968, *Astrophys. Space Sci.* **1**, 429
Truran, J.: 1980, *Nukleonika* **25**, 1472
Wheeler, J.C.: 1977, *Astrophys. Space Sci.* **50**, 125
Woosley, S.E., Weaver, T.A.: 1982, in *Supernovae: A Survey of Current Research*, eds. M.J. Rees and R.J. Stoneham, Reidel, Dordrecht, p. 79